CORROSION SCIENCE AND TECHNOLOGY, Vol.7, No.4(2008), pp.201~207

Spectral Analysis of CO_2 Corrosion Product Scales on 13Cr Tubing Steel

Lin Guan-fa†, Xu Xun-yuan[1], Bai Zhen-quan, and Feng Yao-rong

The Key Laboratory for Mechanical and Environmental Behavior of Tubular Goods, CNPC, Xi'an 710065
[1]PetroChina Tarim Oilfield Compamy, Korla, 841000

CO_2 corrosion product scales formed on 13 Cr tubing steel in autoclave and in the simulated corrosion environment of oil field are investigated in the paper. The surface and cross-section profiles of the scales were observed by scanning electron microscopy (SEM), the chemical compositions of the scales were analyzed using energy dispersion analyzer of X-ray (EDAX), X-ray diffraction (XRD) and X-ray photoelectron spectroscopy (XPS) to confirm the corrosion mechanism of the 13 Cr steel in the simulated CO_2 corrosion environment. The results show that the corrosion scales are formed by the way of fashion corrosion, consist mainly of four elements, i.e. Fe, Cr, C and O, and with a double-layer structure, in which the surface layer is constituted of bulky and incompact crystals of $FeCO_3$, and the inner layer is composed of compact fine $FeCO_3$ crystals and amorphous $Cr(OH)_3$. Because of the characteristics of compactness and ionic permeating selectivity of the inner layer of the corrosion product scales, 13 Cr steel is more resistant in CO_2 corrosion environment.

Keywords *: CO_2 corrosion, corrosion product scale, spectral analysis, 13 Cr steel*

1. Introduction

The carbon dioxide corrosion is one of the main types of oil tube damage and failure in environment of oil and gas exploitation.[1)] The carbon steel and low alloy steel could be resistant to the CO_2 corrosion under low temperature and common pressure condition and can also meet the requirement specified in relative standard.[2),3)] With increasing the depth of the well the temperature and pressure get higher and higher, the corrosion condition becomes more rigorous, which leads to that some advanced steels with good corrosion resistance such as some stainless (304L, 316L, et al) and high Cr steels (HP13Cr type, 18Cr type, 22Cr type, 25Cr type or SAF 2205, et al) have been used in some oil and gas fields,[4)-7)] in spite of the much higher exploiting cost.

Many researches[7)-10)] showed that the corrosion resistance and the price of common 13 Cr steel is between that of common carbon steel and advanced corrosion resistance steel, so it is necessary to research the corrosion resistance characteristic of common 13 Cr steel in the corrosion environment with higher temperature and pressure, and is helpful for petroleum industry to choose the reasonable material used in the corrosion environment and to increase the commercial benefit of the oil fields.

For evaluating the corrosion resistance character of common 13 Cr steel, the CO_2 corrosion product scales on common 13 Cr steel were prepared in autoclave by simulating more serious corrosion environment of oil field, and their chemical compositions were confirmed using spectral analysis associated with analyzing the profile characteristics to infer the forming mechanism of the corrosion scale.

2. Experimental

The tested material is 13 Cr steel with the chemical composition listed in Table 1.

The samples were machined into arc slices of Φ72.0 mm×11.0 mm×3.0 mm (their central angles are all 60°), and the investigated surfaces were polished with sand papers from 120# to 1000#, then put in acetone for removing oil, and dried. The other surfaces were sealed up with silicon rubber NQ-704. The samples were fixed on the outer circumferential surface of a discal clamp with the silicon rubber, placed in a desiccator for 24 h solidified.

The experiment was performed in a 344.4×10^5Pa dynamic autoclave manufactured by Cortest Co.(America)[4)]

† Corresponding author: lingf808@126.com

Table 1. Chemical composition of 13 Cr steel(wt %)

C	Si	Mn	P	S	Cr	Mo	Ni	V	Ti	Cu
0.18	0.33	0.48	0.020	0.001	12.94	0.013	0.10	0.048	0.016	0.013

by fixing the discal clamp with the samples on an autoclave stirrer in the corrosive medium, 5000 mg/L NaCl solution. After being sealed and covered, the autoclave was aerated with N_2 gas to drive O_2 for 6 h, and then aerated with CO_2 for 8h. The testing temperature, CO_2 partial pressure and rotary speed were adjusted to their predefined values. The corrosion experiment lasted for 15d. After that, the corroded samples were washed with water, dried with absolute alcohol, and kept in the other desiccators.

The surface and cross-section morphology of CO_2 corrosion scales were observed with SEM (PHILIPS XL-20), the composition of the scales was analyzed with energy dispersion analysis of X-ray (EDAX), and the X-ray diffraction (XRD) pattern of the scales was investigated by D/max-3C automatic X-ray diffract-meter with a copper K^{α}X-ray source, 40 kV and 100 mA.

The corrosion scale on the corroded surface is analyzed using X-ray photoelectron spectroscopy (XPS, Perkin Elmer, PHI 5000, ESCA) with a set of operating parameters as follows: the magnesium K^{α}X-ray source with a power of 300 W, the pass energy of 89.45 eV for all elements or 71.55 eV for single element through narrow scanning, an analysis area approximately 1.0 mm^2, the vacuum in the test chamber of 2×10^{-8} Pa, and an angle of X-ray incidence of 45°. The binding energies were calibrated by taking C1s peak, 284.6 eV as a criterion. The original surface of the scale was first spattered using argon gas for 10 min. to remove the surface impurity adsorbed from the air by pretreatment, and then the scanning for all elements of the scale was performed from 0 to 1000 eV.

3. Results

3.1 Profile characteristics of CO_2 corrosion product scales on 13 Cr steel

The corrosion product scale formed on the substrate surface of 13 Cr steel is puce and the morphologies of the surface and cross-section of the corrosion scales formed at 110℃ are displayed in Fig. 1. It can be seen from Figs. 1(a) and (b) that the corrosion scales are even, uniform and compact with many fine nicks on the surface of the substrate covered by a thin layer of corrosion scale, which can lead to the conclusion that the corrosion type of 13 Cr steel under the testing condition is uniform corrosion.

There are a few of dispersed corrosion product crystals on the surface of the corrosion scale, which their shape and colour are varied with that in the corrosion product scale close to the metallic substrate (called as the inner layer), and the composition of which should also be different from that in the inner layer as shown in the following compositive analysis. The morphology of the CO_2 corrosion scale formed on 13 Cr steel at 170℃ is showed in Fig. 2, in which the dispersed crystals is more than that

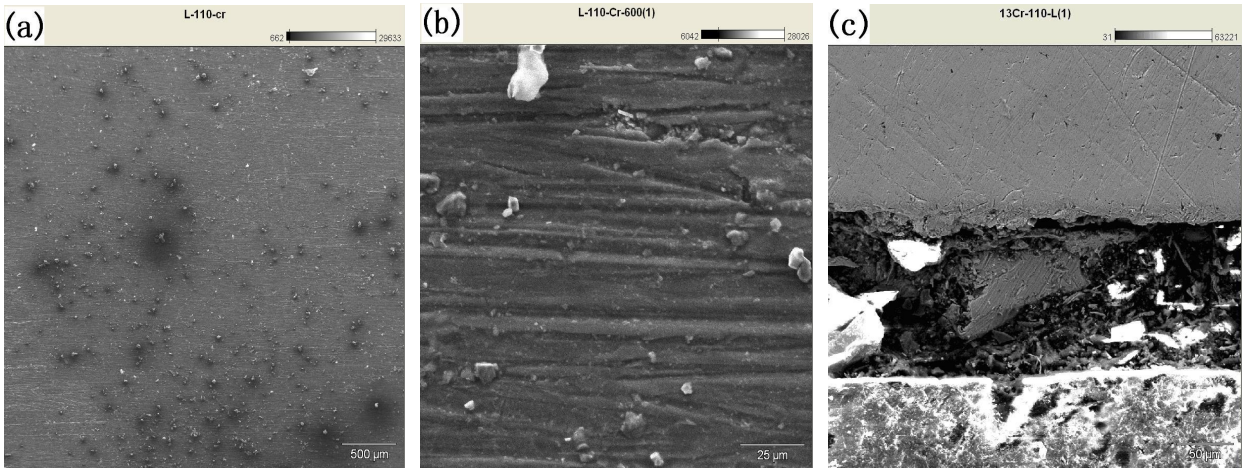

Fig. 1. Morphologies of the surface and the cross-section of the CO_2 corrosion scales on 13 Cr steel at 110℃(a: 25×; b: 600×; c: 400×)

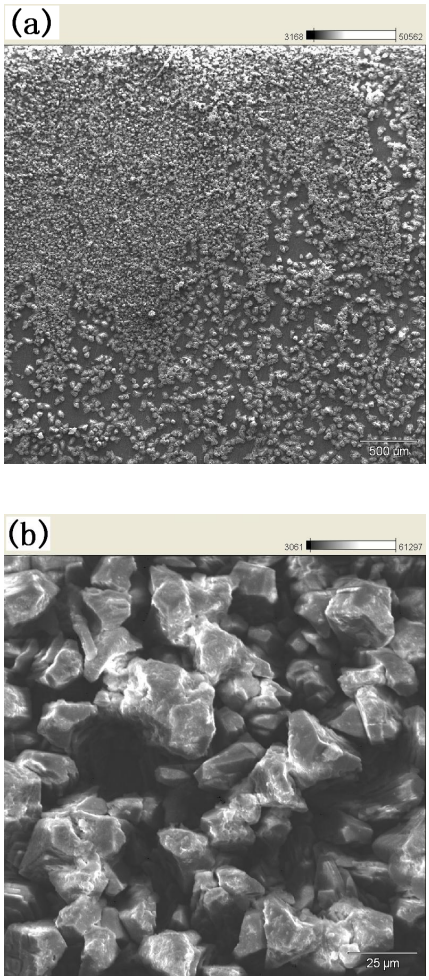

Fig. 2. Surface morphologies of the CO_2 corrosion product scales on 13 Cr steel at 170℃(a: 25×; b: 600×)

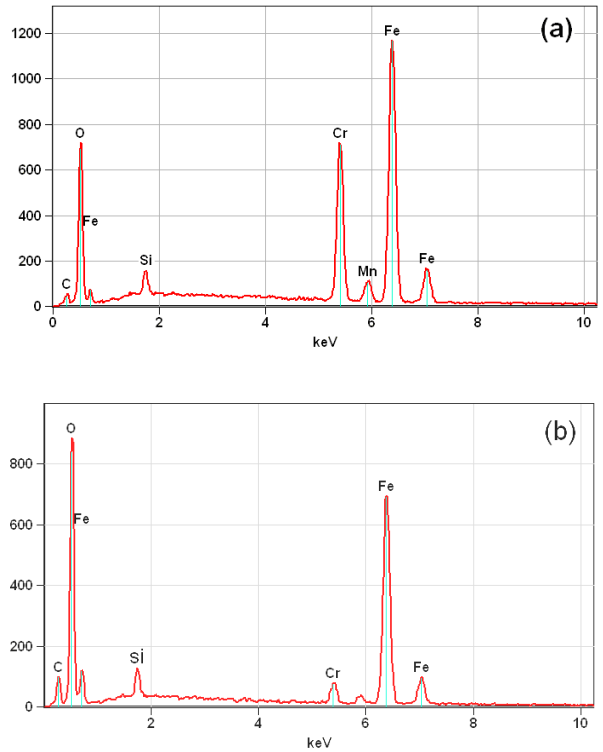

Fig. 3. EDAX analysis of corrosion scale formed on 13 Cr steel at 110℃(a: the inner layer; b: the surface layer)

Table 2. Element percentage of the scale analyzed with EDAX

Element	C	O	Cr	Mn	Fe	Total
Inner layer	7.41	31.16	17.29	0.30	43.84	100
Outer layer	19.61	52.68	1.13	/	26.58	100

in Figs. 1(a) and (b), the area uncovered with the crystals in Fig. 2 is less than that in the latter, but the interspace between the crystals is still very big. All this observation shows that the baffling function of the corrosion scale from corrosion medium is very low, and in fact only the thin inner layer should have good inhibitive property and plays an important role in resisting the permeation of corrosion solution because of its compactnesss. The cross-section structure of the corrosion scale in Fig. 1(c) shows the interface between the steel substrate in the upper and the corrosion scale in the center is even and flat, no sharp hollow or bulgy, from which it can be inferable that the corrosion of 13 Cr steel is the type of uniform corrosion.

2.2 EDAX analysis of CO_2 corrosion product scale

Energy dispersion analysis of X-ray for the corrosion product scale on 13 Cr steel at 110℃ in Fig. 3 shows that there are four elements, i.e. Fe, Cr, O and C, in the inner layer and the surface crystals, in which Fe and Cr come from the substrate of 13 Cr steel, O element from the corrosion medium, and C element mainly from the corrosion medium and a little from the substrate. It is worthwhile to note that Si element is from silicon rubber used as the material sealed the samples and C element comes also from containing carbon impurity imported from the processes of preparing the samples. There exists distinctly a little Mn element in the inner layer in Table 2, because Mn is one of the participators of the anodic corrosive reaction and it is only much less Mn existed in the alloy substrate (0.48%, see Table 1).

The element percentage of CO_2 corrosion product scale on 13 Cr steel at 110℃ analyzed with EDAX is listed in Table 2. It can be seen from the table that the main components in the corrosion scale should be the product of corrosion reaction for Fe and Cr elements, which is proved by the following XRD and XPS analyses as well.

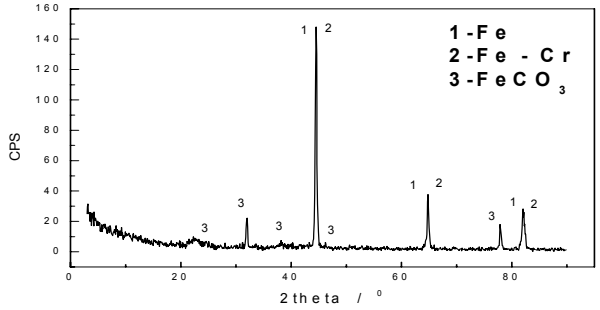

Fig. 4. XRD spectrum of CO_2 corrosion scale formed on the 13 Cr steel at 110℃

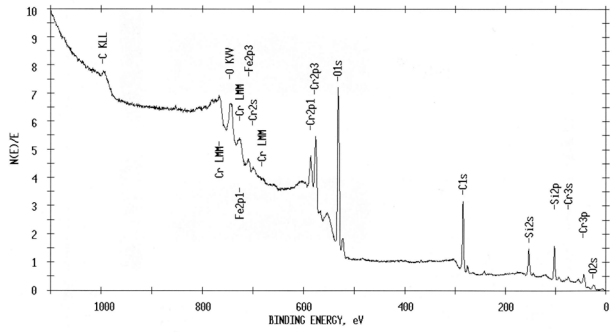

Fig. 5. XPS of all elements in CO_2 corrosion scale

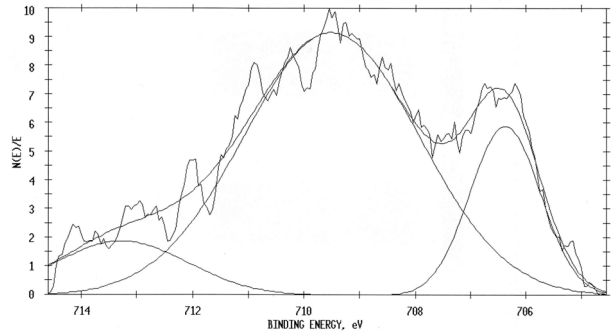

Fig. 6. XPS of Fe element in CO_2 corrosion scale

2.3 XRD analysis of CO_2 corrosion product scale

The XRD spectrum of CO_2 corrosion product scale formed on 13 Cr steel at 110℃in Fig. 4 shows that the main composition of corrosion scale is Fe, Fe-Cr and $FeCO_3$. It is worthwhile to be note that a little protuberant peak located at 22° in the figure is one of the typical characteristics for amorphous compounds in XRD spectrum. Under some reaction condition, Cr element of the substrate may form $Cr(OH)_3$ and its dehydrated product Cr_2O_3. Since $Cr(OH)_3$ is an amorphous compound but Cr_2O_3 is a kind of crystal structure, a protuberant peak appears in the XRD spectrum, which means the existence of the amorphous compound $Cr(OH)_3$ in corrosion product and the area of its peak accords with its content in the scale. Because the area of the protuberant peak is less than that of the other compound's peaks, the proportion of the amorphous $Cr(OH)_3$ is very little in the corrosion scale, which is consistent with the result of EDAX spectral analysis.

2.4 XPS analysis of CO_2 corrosion product scale

X-ray Photoelectron Spectrum (XPS) analysis, which can give a combined spectrum of various electronic sub-shell of each element in the corrosion scale and further the composition of the scale, is one of the impactful methods for analyzing and affirming the chemical composition of corrosion scale and is helpful to confirm and understand the corrosion type and corrosion mechanism of the steel.

Fig. 5 shows XPS of all elements of CO_2 corrosion product scale formed on 13 Cr steel at 110℃. It can be seen from the figure that the corrosion scale contains mainly four kinds of elements, i.e. Fe, Cr, O and C, except Si element as mentioned above of the results of EDAX and XRD analysis. The element content of the corrosion scale tested by XPS is listed in Table 3. The measured result is various with that in Table 2, which is caused from the fact that EDAX tests at a dot, but XPS belongs to an area and an average value as taking its result.

The narrow XPS spectrum is then analyzed for each element to confirm further its chemical combining state in the scale. The figure of XPS of Fe element in CO_2 corrosion product scale formed on 13 Cr steel at 110℃ in Fig. 6 shows three standard peaks located at 706.38 eV, 709.51 eV and 713.27 eV, which correspond to Fe^0, Fe^{2+} and the concomitant peak of Fe element, respectively. As a little pure iron examined by XPS in the scale comes from the rudimental scrap iron produced in the process of machining steel samples and a few substrate grains enwrapped in the scale, the Fe element in the scale on 13 Cr steel exists in the form of $FeCO^3$.

Table 3. Element content of corrosion scale tested by XPS (wt%)

Element	C	O	Cr	Fe	Total
Content	44.54	43.08	2.28	10.10	100

Fig. 7 shows XPS of Cr element of CO_2 corrosion product scale formed on 13 Cr steel at 110℃ which contains three standard peaks located at 574.15 eV, 576.41 eV and 578.51 eV corresponding to Cr^0, Cr^{+3} and Cr^{+6} chemical combining state, respectively. The peak area of Cr^0 or Cr^{+6} chemical combining state is less than that of Cr^{+3}, so Cr element in the scale might exist mainly as Cr^{+3} compound. From the test result of XRD for the scale, the Cr^{+3} compound may be the amorphous $Cr(OH)_3$ but not the crystal

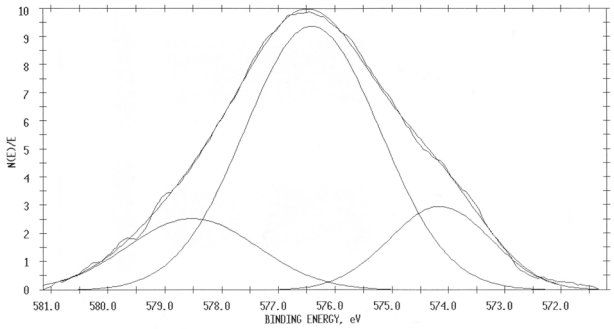

Fig. 7. XPS of Cr element in CO_2 corrosion scale

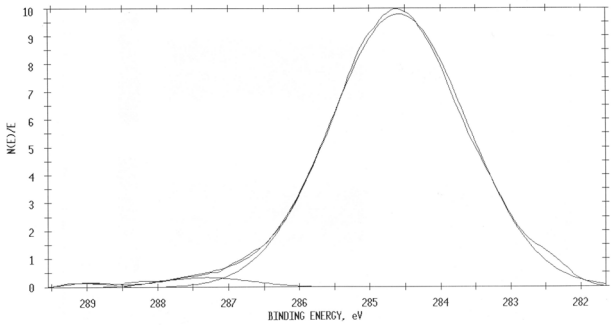

Fig. 8. XPS of C element in CO_2 corrosion scale

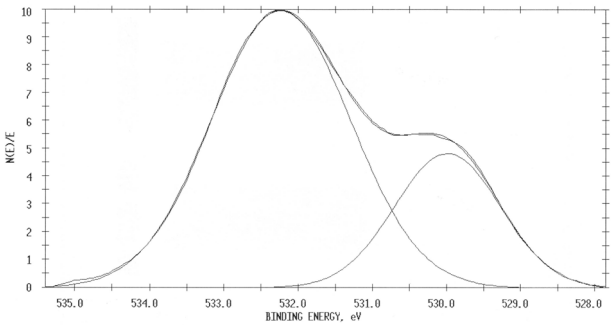

Fig. 9. XPS of O elements in CO_2 corrosion scale

Cr_2O_3. Cr^{+6} chemical combining state exists maybe in the combining form of CrO_3 or $Cr_2O_7^{2-}$, but their content in the scale is limited.

Fig. 8 shows XPS of C element of CO_2 corrosion product scale formed on 13 Cr steel at 110℃. It is seen from the figure that the energy spectrum can be simulated from three standard peaks located at 288.97 eV, 287.30 eV and 284.59 eV, which may correspond with CO_3^{2-} or HCO_3^-, simple organic compounds and metallic carbide. Here, the metallic carbide should be Fe_3C or $(Fe, Cr)_7C_3$ from the substrate of 13 Cr steel, organic compounds should be absorbed in the process of sealing, washing, drying, storing of the corrosion samples, so C element of the corrosion scale exists in the form of carbonate or bicarbonate.

XPS of O element in Fig. 9 can be imitated from three standard peaks located at 532.24 eV and 529.99 eV correspond to hydrate or oxide of Fe and Cr elements respectively. The content of Cr hydrate is more than that of oxide, and the ferrous oxide or hydrate is very little.

4. Discussion

In the CO_2 Corrosion environment, the alloying elements of 13 Cr steel can produce the following anodic reactions[11),12)]:

$$Fe \rightarrow Fe^{2+} + 2e \quad (1)$$

$$Cr \rightarrow Cr^{3+} + 3e \quad (2)$$

The alloy contains Mn and Ni elements which take also part in such anodic reactions, as mentioned above in the result of the EDAX. There contains commonly the following reactive process in the corresponding cathodal CO_2 corrosion reactions[11),12)]:

$$CO_2 + H_2O \leftrightharpoons H_2CO_3 \quad (3)$$

$$2H_2CO_3 + 2e \leftrightharpoons H_2 + 2HCO_3^- \quad (4)$$

$$2HCO_3^- + 2e \rightarrow H_2 + 2CO_3^{2-} \quad (5)$$

$$2H^+ + 2e \rightarrow H_2 \quad (6)$$

In neutral or weak acidic corrosion environment, the positive and negative ions in above reactions can form corrosion products through the following reactions[11),12)]:

$$Fe^{2+} + 2HCO_3 \rightarrow Fe(HCO_3)_2 \rightarrow FeCO_3 + CO_2 + H_2O \quad (7)$$

$$Fe^{2+} + CO_3^{2-} \rightarrow FeCO_3 \quad (8)$$

$$Cr^{3+} + 3H_2O \rightarrow Cr(OH)_3 \rightarrow Cr_2O_3 + H_2O \quad (9)$$

The corrosion reaction of Mn^{2+} ion of forming the corrosion product is similar to that of Fe^{2+} ion, but as a little Mn element in the substrate, only a little Mn^{2+} corrosion product may also be included in the CO_2 corrosion product scale of 13 Cr steel.

With increasing the temperature or decreasing the CO_2 partial pressure in the corrosion process, the ferrous corrosion product can form its oxides through the following reactions[13)]:

$$FeCO_3 \rightarrow FeO + CO_2 \quad (10)$$

$$4FeO + O_2 \rightarrow 2F_2O_3 \quad (11)$$

$$3FeO + CO_2 \rightarrow Fe_3O_4 + CO \quad (12)$$

$$3FeO + H_2O \rightarrow Fe_3O_4 + H_2 \quad (13)$$

$$4Fe_3O_4 + O_2 \rightarrow 6Fe_2O_3 \quad (14)$$

The reaction (10) can occur below 100℃, but it is limited only at high CO_2 partial pressure (p_{CO2}=2MPa); the reactions (11)~(14) follow the reaction (10), but the reactions (12) and (13) occur in the anoxic condition, and the reactions (11) and (14) in the aerobian condition. The total amount of ferreous oxides in the corrosion scale on 13 Cr steel is so very little that they can't be measured with XRD spectrum. Likewise, it is seen from the result of XRD analysis that chromic oxides in the scale are very little. The corrosion scale formed on 13 Cr steel at 110℃ is consisted of $FeCO_3$ and $Cr(OH)_3$, with mainly bigger crystal of $FeCO_3$ in the surface layer and amorphous $Cr(OH)_3$ besides $FeCO_3$ crystals in the inner layer close to the substrate, and that $Cr(OH)_3$ exists only almost in the inner layer.

Under the testing condition, when $FeCO_3$ and $Cr(OH)_3$ have formed in the corrosion medium, as the two compounds have very small solubility in the medium, the two corrosion products can deposit on the surface of the substrate and also the other surface in autoclave, which results in the corrosion rate of the substrate to be decreased into a small stable value after some time.[14] As the corrosion rate at initial corrosion stage is higher, the size of the deposited corrosion product grains is smaller; the corrosion rate at the ending corrosion stage is lower, the size of the grains is bigger. At the same time the grains formed at the ending stage deposit on the surface of corrosion layer formed in initial corrosion process, so the corrosion product scale is with double-layer structure, in which the crystals in the surface layer is more bulky and the grains in the inner layer is finer.[14] Because of the amorphous $Cr(OH)_3$ in the inner layer and its ionic permeating selectivity,[15] this two important aspects are helpful to enhance the compactness of the corrosion product scale, which is one of primary reasons why 13 Cr steel has good corrosion resistance in CO_2 environment.

5. Conclusion

1) Under the testing condition, the CO_2 corrosion product scale formed on 13 Cr steel is with double layers structure, in which the thin compact inner layer consists of fine grains and the thick loose surface layer of bulky crystals.

2) The CO_2 corrosion product scale contains mainly four elements: Fe, Cr, C and O, but the compositions of the two layers are obviously different, the amorphous $Cr(OH)_3$ besides $FeCO_3$ in the inner layer and mainly $FeCO_3$ crystals in the outer layer.

3) Ferreous oxides aren't all discovered in the two layers of CO_2 corrosion scale on 13 Cr steel, which results from that CO_2 partial pressure in the testing condition is so high that the decomposing reaction of $FeCO_3$ is restrained.

4) The amorphous $Cr(OH)_3$ in the inner layer helps to enhance the compactness and selectivity of the corrosion product scale, which is one of main reasons why 13 Cr steel has good corrosion resistance in CO_2 corrosion environment.

Acknowledgement

Financial support from the National Natural Science Foundation of China (No. 50231020) and Applied Basic Research Project of China National Petroleum Corporation (No. 06A40302) is gratefully acknowledged.

References

1. J. S. Zheng and Z. P. Lu, *Acta petrolei sinica*, **16**, 134 (1995).
2. M. L. Yan, G. X. Zhao, and M. X. Lu, *Materials Protection*, **32**, 27 (1999).
3. G. X. Zhao, M. L. Yan, M. X. Lu, and P. Q. Li, *Corrosion Science and Protection Technology*, **12**, 240 (2000).
4. D. Q. Tong and J. Wu, *Journal of Iron and Steel Rearch*, **3**, 1 (1991).
5. J. Wang, Z. Q. Bai, G. F. Lin, and H. L. Li, *Materials Development and Application*, **20**, 26 (2005).
6. Z. B. Chen, D. Q. Song, X. Y. Tang, and Q. Zhang, *Gas and Oil*, **24**, 1 (2006).
7. X. H. Dong, G. X. Zhao, Y. R. Feng, and Y. Jiang, *Oil Field Equipment*, **32**, 1 (2003).
8. X. H. Lu, G. X. Zhao, Z. H. Fan, Y. Q. Yang, C. F. Chen, and M. X. Lu, *Materials Protection*, **37**, 34 (2004).
9. A. Ikeda, S. Mukai, and M. Ueda, *Corrosion*, **41**, 185 (1985).
10. X. H. Lu, G. X. Zhao, Y. Q. Yang, J. Z. Ma, C. F. Chen, and M. X. Lu, *Materials Engineering*, **10**, 16 (2004).
11. C. Waard and D. E. Millliams, *Corrosion*, **31**, 177 (1975).
12. E. Dayalan, G. Vani, and J. R. Shadley, Corrosion/95, paper 118, NACE, Houston (1995).

13. J. K. Heuer and J. F. Stubbins, *Corrosion Science*, **41**, 1231 (1999).
14. G. Lin, M. Zheng, Z. Bai, and X. Zhao, *Corrosion*, **62**, 501 (2006).
15. A. R. Brooks, C. R. Clayton, K. Doss, and Y. C. Lu, *Journal of Electrochemical Society*, **133**, 2459 (1986).